

Surface properties of the refractory metal-nitride semiconductor ScN: Screened-exchange LDA-FLAPW investigations

C. Stampfl,¹ R. Asahi,^{1,2} and A. J. Freeman¹

¹*Department of Physics and Astronomy, Northwestern University, Evanston, Illinois 60208-3112*

²*Toyota Central R&D Laboratories, Inc., Nagakute, Aichi 480-1192, Japan*

(Received 24 September 2001; revised manuscript received 7 December 2001; published 15 April 2002)

Density-functional theory calculations employing the screened-exchange local-density approximation (SX-LDA) with the full potential linearized augmented plane-wave method have recently shown that the relatively unexplored refractory nitrides ScN, YN, and LaN are semiconductors. For the ScN(001) surface, the present calculations predict that the ideal-relaxed surface has the lowest formation energy for most of the range of the allowed chemical potentials—and is semiconducting—while N-deficient structures, which are predicted to form for Sc-rich conditions, are metallic in nature. Compared to the LDA surface-state band structures, the SX-LDA selectively *pushes down* the valence bands for the Sc-terminated surface and *pushes up* the conduction bands for the N-terminated structure.

DOI: 10.1103/PhysRevB.65.161204

PACS number(s): 68.35.-p, 71.20.-b

The early transition-metal mononitrides crystallize in the rocksalt structure and exhibit extreme and unique physical properties of hardness, brittleness, high melting point, and in some, superconductivity. They have technological applications in the area of, for example, hard coatings for cutting tools¹ and possible potential for applications in magnetic recording and sensing.^{2,3} These materials are metallic, with the exception of ScN (and possibly YN and LaN), for which there have been conflicting reports in the literature: Early experiments indicated that ScN is an indirect semimetal,⁴ as supported by density-functional theory (DFT) calculations performed within the local-density approximation (LDA).⁵ More recent experiments, however, report that it is a semiconductor,⁶⁻⁹ confirming recent theoretical investigations: In our earlier work using the screened-exchange (SX)-LDA approach¹⁰ we reported that ScN, YN, and LaN are indirect semiconductors, with gaps of 1.58, 0.85, and 0.75 eV, respectively; within the LDA they are all semimetals. Also two other very recent calculations of the band structure of ScN have been performed, one which includes quasiparticle corrections¹¹ and the other employing the exact-exchange formalism,⁸ where both also find it is an indirect semiconductor; the reported band gaps are 0.9 and 1.6 eV, respectively. In Ref. 11 it was also concluded that GdN is a narrow band-gap semiconductor with a gap of 0.7–0.85 eV. Therefore these early transition-metal (refractory) nitrides represent a *different system of semiconducting materials*.

The prospect of additional semiconducting III-N materials to those of technologically important GaN, AlN, and InN [e.g., in relation to optoelectronic (and high temperature) devices such as blue laser diodes¹²] opens up the possibility of their complementary use in such GaN-based applications. If this is so, then the nature of their surfaces becomes an important consideration; for example, the electronic properties, stability, and the ability to form atomically smooth surfaces and interfaces.

Clearly to investigate the electronic properties of these materials, it is necessary to use a method that provides an accurate description of the excited-state properties. In this paper, we report DFT full potential linearized augmented

plane-wave (FLAPW) calculations^{13,14} using the recently implemented SX-LDA for bulk¹⁵ and for superlattices and film geometries,¹⁶ as well as the usual LDA.¹⁷ In particular, we investigate the surface atomic and electronic properties of ScN(001), which has a near perfect lattice match to GaN (<0.3%). The SX-LDA approach has been shown to yield good agreement of the calculated band gaps with experimental values.^{15,16,18,19} It is less computationally demanding than the GW method²⁰ and also permits self-consistent determination of electronic structures as well as eigenfunctions.^{15,16} Proposed by Bylander and Kleinman,¹⁸ Seidl *et al.*¹⁹ who showed that the method can be introduced as a particular case of the generalized Kohn Sham (KS) framework, the essence being that the energy functional can include some part of the *interacting* energy functional as well as the non-interacting one (as employed in the KS scheme). The single-particle equation is then written as

$$\left(\frac{-\hbar^2}{2m} \nabla^2 + v_{eff}(\mathbf{r}) \right) \psi_i(\mathbf{r}) + \int d\mathbf{r}' v_{sx}^{NL}(\mathbf{r}, \mathbf{r}') \psi_i(\mathbf{r}') - v_{sx}^L(\mathbf{r}) \psi_i(\mathbf{r}) = \epsilon_i^{sx} \psi_i(\mathbf{r}), \quad (1)$$

where $v_{eff}(\mathbf{r})$ is the effective potential from the LDA, and v_{sx}^{NL} and v_{sx}^L are nonlocal and local screened exchange potentials, respectively, which are obtained by employing Thomas-Fermi screening (see, e.g., Refs. 15 and 16). That the SX-LDA yields an improved description of the band gap can be understood in that the derivative of the discontinuity of the exchange-correlation energy, which is missing in the Kohn-Sham band gap, is intrinsically involved in the SX-LDA formalism.

The technical details of our calculations are as follows: We treat the core states fully relativistically and the valence states scalar relativistically, and use angular momenta up to $l=8$ in the muffin-tin spheres for both the wave functions and charge density in the self-consistent cycles. We use muffin-tin radii of $R_N=1.5$ and $R_{Sc}=2.41$ bohrs for the N and Sc atoms, respectively, and 21, 6, and 6 \mathbf{k} points in the irreducible part of the surface Brillouin zone (IBZ) for the

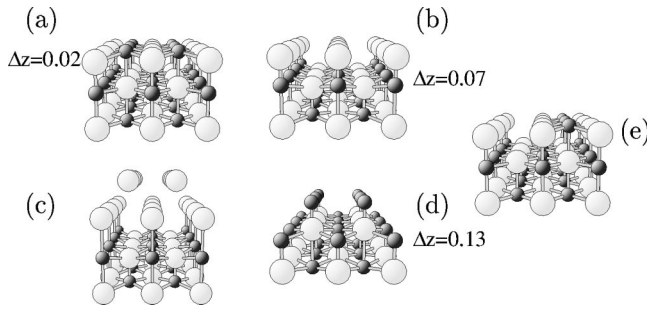


FIG. 1. Surface structures of the (1×1) -ScN(001) (a) ideal-, (b) Sc-, (c) 2Sc-, (d) N-terminated surfaces, and (e) the (2×1) N-deficient (vacancy) structure. The magnitude of rumplings in various atomic layers is indicated (in Å). Large and small spheres indicate Sc and N atoms, respectively.

(1×1) LDA, the (1×1) SX-LDA,²¹ and the (2×1) LDA structures, respectively. The cutoff energy for the plane-wave expansion in the interstitial region is 18.5 Ry. Nine ScN(001) layers are used to model the surface within the film geometry. (In this approach with a single slab, it is not necessary to impose an artificial periodicity of the slab in the z direction—as is done with other approaches.) We relax the positions of all the atoms until the forces are less than 2 mRy/a.u.

Recent scanning tunneling microscopy (STM) studies²² have demonstrated that under N-rich conditions, atomically flat (1×1) -ScN(001) surfaces can be grown. The STM images showed only one feature in the (1×1) surface unit cell. Given that there are two atoms (one Sc and one N) in the ideal (1×1) -ScN(001) surface unit cell, this result could be due to missing N or Sc atoms, or it could be an electronic effect of the ideal surface; neither one could be concluded from the study. A subsequent STM study²³ of surfaces grown under Sc-rich conditions shows noticeably different behavior; in particular, spiral growth with very “smooth” (in terms of corrugation) surfaces, as well as pits. It was suggested that they have metallic character and may be Sc rich in stoichiometry.

In order to investigate possible surface structures that may form under various conditions, we consider the following geometries: (1×1) ideal-, Sc-, 2Sc-, and N-terminated structures, as well as a (2×1) N-vacancy structure (see Fig. 1). We note that the STM studies showed no indication of a (2×1) periodicity and we study this structure only as a model for an intermediate Sc-rich (N-deficient) surface. In addition, we investigated the Sc- and N-terminated structures, but with a larger (2×1) periodicity to allow for the possibility of atom pairing should it be energetically favored; this, however, was found not to be the case. For the unreconstructed surface [Fig. 1(a)], there is only a small rumpling (0.02 Å) of the surface Sc and N atoms, with the Sc atoms moving slightly inwards and the N atoms slightly outwards. This is in very good agreement with calculations by Takeuchi who obtained a value of (0.03 Å) as described in Ref. 23. The other structures exhibit somewhat larger relaxations as seen from Fig. 1.

To compare the relative stability of the surfaces, we calculate the surface formation energy,

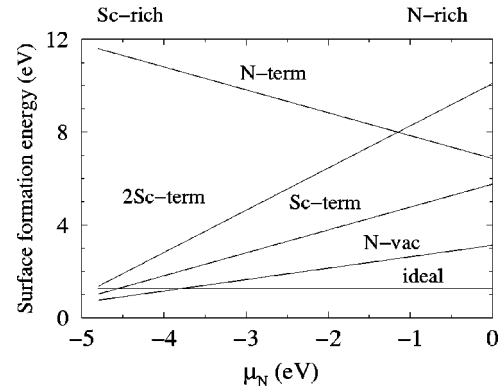


FIG. 2. Surface formation energies for the (1×1) ideal-relaxed, N-, 2Sc-, and Sc-terminated surfaces, and the (2×1) N-deficient (vacancy) structure versus the N chemical potential, μ_N , which spans the range of the heat of formation of ScN—calculated to be 4.8 eV (Ref. 10). The chemical potential of N in N_2 , μ_{N_2} , is taken as the energy zero.

$$\sigma_{\text{surf}} = 1/2(E_{\text{surf}}^{\text{tot}} - nE_{\text{bulk}}^{\text{tot}} + 2\mu_X), \quad (2)$$

where $E_{\text{surf}}^{\text{tot}}$ and $E_{\text{bulk}}^{\text{tot}}$ are the total energies of the surface system and of a bulk unit of ScN, respectively, and n is the number of Sc (and N) atoms in the corresponding ideal surface slab. The chemical potential of atom X (here Sc or N), denoted as μ_X , accounts for atoms that may be added to, or taken from, the ideal surface and depends on the experimental conditions under which the material is grown. Assuming both species are in thermal equilibrium with bulk ScN, we have $\mu_{\text{Sc}} + \mu_{\text{N}} = \mu_{\text{ScN}}$, where μ_{ScN} is the chemical potential of ScN. Furthermore, the chemical potentials must satisfy the boundary conditions: $\mu_{\text{N}} < 1/2\mu_{N_2}$ and $\mu_{\text{Sc}} < \mu_{\text{Sc}(\text{bulk})}$. For nitrogen-rich conditions we set $\mu_{\text{N}} = 1/2\mu_{N_2}$ and for scandium-rich conditions, $\mu_{\text{Sc}} = \mu_{\text{Sc}(\text{bulk})}$. To consider conditions between these two extremes, we also have $\mu_{\text{N}} > \mu_{\text{ScN}} - \mu_{\text{Sc}(\text{bulk})}$ and $\mu_{\text{Sc}} > \mu_{\text{ScN}} - 1/2\mu_{N_2}$, and with the heat of formation, $\Delta H_f^0 = \mu_{\text{Sc}(\text{bulk})} + 1/2\mu_{N_2} - \mu_{\text{ScN}}$, we obtain for the range of the nitrogen chemical potential, $-\Delta H_f^0 < \mu_{\text{N}} - 1/2\mu_{N_2} < 0$.

The surface formation energies for the surfaces considered as a function of the nitrogen chemical potential are shown in Fig. 2. It can be seen that the N-terminated structure is energetically very unfavorable. This surface exhibits a magnetization with the uppermost N atoms having a magnetic moment of $1.6 \mu_B$. The ideal-relaxed surface (which is nonmagnetic) is the most stable one for most of the range of the chemical potential ($\sigma_{\text{ideal}} = 1.26$ eV). For Sc-rich conditions, however, the N-deficient (“N-vac”) (2×1) structure is energetically most favorable ($\sigma_{\text{N-vac}} = 0.77$ eV). It is interesting to note that for strongly Sc-rich conditions, the pure (1×1) -Sc terminated structure is also more favorable than the ideal-relaxed surface ($\sigma_{\text{Sc-term}} = 1.03$ eV). This surface is found to exhibit a small magnetization of the uppermost Sc atoms of $0.2 \mu_B$ —which is interesting since neither bulk

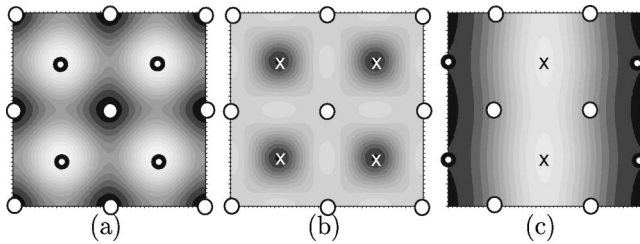


FIG. 3. STM simulations for the (1×1) (a) ideal- and (b) Sc-terminated surfaces, and (c) the (2×1) N-vacancy surface. The area in each case is the same and corresponds to that of a (2×2) cell. Light and dark circles mark the positions of Sc and N atoms, respectively, and crosses indicate the positions of missing top-layer N atoms.

Sc or bulk ScN are magnetic. We also performed spin-polarized calculations for the (2×1) -N-vacancy structure and found a very small magnetic moment of $0.04 \mu_B$ on the uppermost Sc atoms.

On the basis of the calculated surface energies, we can predict that the ideal-relaxed surface is the one which the STM study investigated, since the surface was created under N-rich conditions.²² To explore this further, we performed a simulation of the STM image by integrating the electron density in the energy window from -2 eV to E_F . The result is shown in Fig. 3(a) where the cross-section is in the (001) plane at ≈ 3 Å above the centers of the uppermost atoms. It can be seen that there is only one feature in the surface unit cell, consistent with the experimental result. The maximum of intensity (light region) corresponds to the position of the N atom. We note that in the experiments the samples were reportedly n type, which could be due to impurities or N vacancies (which we find are donors, see below), so that E_F may be close to the conduction-band minimum. A simulation integrating the energies from E_F to 2 eV (i.e., corresponding to states at the bottom of the conduction band) show that in this case the image is just *opposite*, namely, the most intense features correspond to the Sc atoms. The result for the Sc-terminated surface is shown in Fig. 3(b). Here the high intensity region is more diffuse and spreads on, and in-between, the Sc atoms. This reflects the more delocalized, metallic nature of the surface, as will be seen from the surface band structure below. Figure 3(c) shows the result for the (2×1) N-vacancy surface. It can be seen that there is a bright stripe and this corresponds to the region where the N atoms are missing [see Fig. 1(e)], i.e., between the Sc atoms where metallic bonding occurs.

To obtain further insight into the electronic nature of these surfaces, we show in Fig. 4 the SX-LDA band structures for the (1×1) ideal-relaxed-, Sc-, and N-terminated structures, and for comparison the corresponding LDA results. It can be seen from the SX-LDA result that the bulk-terminated surface [Fig. 4(a)] is semiconducting, i.e., there are no states in the band gap. For the Sc-terminated surface, the situation is quite different with the presence of surface states in the gap. In particular, the appearance of the lower state extending parabolically upwards from the valence-band maximum at the $\bar{\Gamma}$ point is free-electron-like, and it joins a number of rather flat partially occupied states. These give rise to a rela-

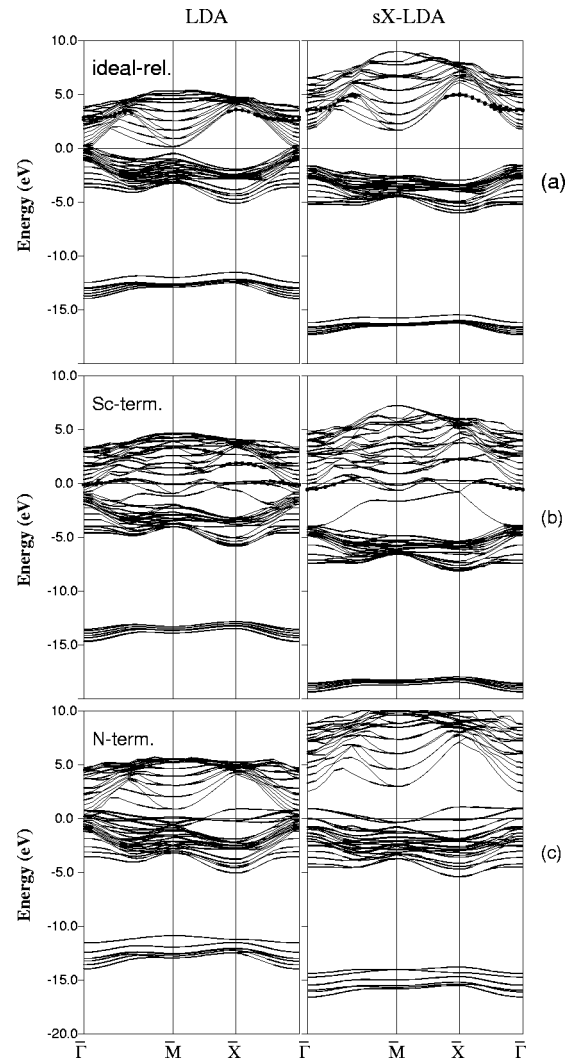


FIG. 4. Surface band structures of (1×1) -ScN(001): (a) ideal-, (b) Sc-, and (c) N-terminated surfaces, as calculated using LDA (left) and SX-LDA (right). The dots indicate that there is some contribution from vacuum states.

tively high density of states (DOS) at E_F . The surface band structure of the (2×1) -N-vacancy structure (not shown) also exhibits a largely occupied surface state band. In this case, however, there are no flat partially occupied surface-derived states at E_F . This results in a lowering of the DOS at the E_F and explains the lower surface formation energy. We note that the nearest-neighbor top-layer Sc-Sc distance of the (1×1) -Sc-terminated structure is only 1.2% smaller than in bulk hexagonal Sc metal, and only 2.0% greater than the equilibrium Sc-Sc distance in a free-standing Sc layer, thus enabling a good metallic bonding without the necessity of reconstruction or significant relaxations. The N-terminated surface [Fig. 4(c)] exhibits quite localized, partially occupied surface states just above the valence bands, which are of N- $2p$ nature. These unsaturated bonds give rise to a high DOS at E_F and a high surface formation energy.

From a methodological point of view, it is interesting to note that the SX-LDA selectively *pushes down* the valence bands for the Sc-terminated surface, keeping the relative po-

sitions between conduction bands and surface states constant, while it *pushes up* the conduction bands for the N-terminated surface. This demonstrates the difficulty in attempting to anticipate in which manner the bands would move, up or down, by just considering the LDA band structure. A similar conclusion was drawn recently for the case of defect levels in semiconductors through comparison of DFT-LDA and calculations including self-interaction and relaxation corrections.²⁴ The Fermi surfaces, however, are relatively similar for the LDA and SX-LDA results, as expected.

To investigate the possibility of thicker films containing N vacancies, we calculated the bulk N-vacancy formation energy (in the neutral charge state) using an 18-atom supercell with two vacancies (corresponding to a Sc to N ratio of 1.25, or vacancy concentration of 0.11), again with full atomic relaxation. For comparison, we also considered the case of the Sc vacancy. For the N (Sc) vacancy, the surrounding four Sc (N) atoms relax radially outwards by 3.2% (5.8%). The vacancy formation energy is calculated in an analogous manner to Eq. (2), except here $E_{\text{surf}}^{\text{tot}}$ is replaced by $E_{\text{defect}}^{\text{tot}}$, the total energy of the defect cell. For Sc-rich conditions, the N-vacancy formation energy is small (and negative, i.e., exothermic), namely, -0.42 eV and for N-rich conditions it is large, 4.32 eV. This indicates that for more Sc-rich conditions, N vacancies can readily form. The Sc-vacancy forma-

tion energy is notably larger, namely, 10.71 and 5.97 eV for Sc- and N-rich conditions, respectively. Thus the probability of Sc vacancies (in the neutral charge state) is much lower. On investigating the electronic structure of the N and Sc vacancies, which we also calculated using a larger 32-atom cell, we find that the former are donors and the latter acceptors, similarly to the III-V nitrides, GaN, AlN, InN.

Our results can therefore be summarized as follows: We predict that the ScN(001) surface, when grown under N-rich conditions, has the (1×1) ideal-relaxed structure which is semiconducting with no states in the band gap; for more Sc-rich conditions, N deficient (or vacancy) surface structures should become stable which are metallic in nature. We also find for Sc-rich conditions, that the (neutral) bulk N vacancy, which is a donor, has a low formation energy, indicating that thicker, N-deficient films may form. These results appear to be consistent with recent STM studies.^{22,23}

This work was supported by the Department of Energy (Grant No. DE-F602-88ER45372) and computing resources provided at NERSC. We thank A. R. Smith, D. Gall, M. E. Kordesch, and W. R. L. Lambrecht for sending preprints prior to publication, and A. R. Smith and N. Newman for stimulating discussions.

¹S. Vepřek, J. Vac. Sci. Technol. A **17**, 2401 (1999).

²H. Yang, H. Al-Britthen, A.R. Smith, J.A. Borchers, R.L. Cappelletti, and M.D. Vaudin, Appl. Phys. Lett. **78**, 3860 (2001).

³A. Madan, Y. Wang, S.A. Barnett, C. Engström, H. Ljungcrantz, L. Hultman, and M. Grimsditch, J. Appl. Phys. **84**, 776 (1998).

⁴G. Travaglini, F. Marabelli, R. Monnier, E. Kaldis, and P. Wachter, Phys. Rev. B **34**, 3876 (1986).

⁵R. Monnier, J. Rhyner, T.M. Rice, and D.D. Koelling, Phys. Rev. B **31**, 5554 (1985).

⁶P.J. Dismukes, M.W. Yim, and S.V. Ban, J. Cryst. Growth **13/14**, 365 (1972).

⁷T.D. Moustakas, R.J. Molnar, and J.P. Dismukes, Electrochem. Soc. Proc. **96**(11), 197 (1996), and references therein.

⁸D. Gall, M. Städele, K. Järrendahl, I. Petrov, P. Desjardins, R.T. Haasch, T.-Y. Lee, and J.E. Greene, Phys. Rev. B **63**, 125119 (2001), and references therein.

⁹X. Bai, D.M. Hill, and M.E. Kordesch, in *Wide-Bandgap Semiconductors for High-Power, High Frequency and High-Temperature and High-Temperature Applications—1999*, edited by S. Binari, A. Burk, M. Mollock, and C. Nguyea, M. R. S. Symposia Proceedings No. **572** (Materials Research Society, Pittsburgh, 1999), p. 529.

¹⁰C. Stampfl, W. Mannstadt, R. Asahi, and A.J. Freeman, Phys. Rev. B **63**, 155106 (2001).

¹¹W.R.L. Lambrecht, Phys. Rev. B **62**, 13 538 (2000).

¹²F.A. Ponce and D.P. Bour, Nature (London) **386**, 351 (1997), and references therein.

¹³E. Wimmer, H. Krakauer, M. Weinert, and A.J. Freeman, Phys. Rev. B **24**, 864 (1981).

¹⁴A. Canning, W. Mannstadt, and A.J. Freeman, Comput. Phys. Commun. (2000) **130**, 233 (2000).

¹⁵R. Asahi, W. Mannstadt, and A.J. Freeman, Phys. Rev. B **59**, 7486 (1999).

¹⁶R. Asahi, W. Mannstadt, and A.J. Freeman, Phys. Rev. B **62**, 2552 (2000).

¹⁷L. Hedin and B.I. Lundqvist, J. Phys. C **4**, 2064 (1971).

¹⁸B.M. Bylander and L. Kleinman, Phys. Rev. B **41**, 7868 (1990).

¹⁹A. Seidl, A. Görling, P. Vogel, J.A. Majewski, and M. Levy, Phys. Rev. B **53**, 3764 (1996).

²⁰L. Hedin, Phys. Rev. **139**, A796 (1965).

²¹For calculations of the band structure, the smaller \mathbf{k} -point set is sufficient, whereas the energetics are more sensitive.

²²H. Al-Britthen and A.R. Smith, Appl. Phys. Lett. **77**, 2485 (2000).

²³A.R. Smith, H. Al-Britthen, D.C. Ingram, and D. Gall, J. Appl. Phys. **90**, 1809 (2001).

²⁴C. Stampfl, C.G. Van de Walle, D. Vogel, P. Krüger, and J. Pollmann, Phys. Rev. B **61**, R7846 (2000).